Received: 14 May 2019 | Revised: 6 August 2019 | Accepted: 6 August 2019

DOI: 10.1002/mc.23103

Molecular Carcinogenesis WILEY

RESEARCH ARTICLE

Macrophage HIF-2α regulates tumor-suppressive Spint1 in the tumor microenvironment

Rosa M. Susen[1] | Rebekka Bauer[1] | Catherine Olesch[1] | Dominik C. Fuhrmann[1] | Annika F. Fink[1] | Nathalie Dehne[1] | Arpit Jain[2] | Ingo Ebersberger[2,3] | Tobias Schmid[1] | Bernhard Brüne[1,4,5,6]

[1]Institute of Biochemistry I, Faculty of Medicine, Goethe-University Frankfurt, Frankfurt, Germany

[2]Applied Bioinformatics Group, Institute of Cell Biology and Neuroscience, Goethe-University Frankfurt, Frankfurt, Germany

[3]Senckenberg Biodiversity and Climate Research Centre (BiK-F), Frankfurt, Germany

[4]German Cancer Consortium (DKTK), Partner Site Frankfurt, Frankfurt, Germany

[5]Frankfurt Cancer Institute, Goethe-University Frankfurt, Frankfurt, Germany

[6]Project Group Translational Medicine and Pharmacology TMP, Fraunhofer Institute for Molecular Biology and Applied Ecology, Frankfurt, Germany

Correspondence
Bernhard Brüne, Institute of Biochemistry I, Faculty of Medicine, Goethe-University Frankfurt, Theodor-Stern-Kai 7, 60590 Frankfurt, Germany.
Email: b.bruene@biochem.uni-frankfurt.de

Funding information
Deutsche Forschungsgemeinschaft, Grant/Award Number: SFB815 - project A8 (to BB)

Abstract

In solid tumors, tumor-associated macrophages (TAMs) commonly accumulate within hypoxic areas. Adaptations to such environments evoke transcriptional changes by the hypoxia-inducible factors (HIFs). While HIF-1α is ubiquitously expressed, HIF-2α appears tissue-specific with consequences of HIF-2α expression in TAMs only being poorly characterized. An E0771 allograft breast tumor model revealed faster tumor growth in myeloid HIF-2α knockout (HIF-2α$^{LysM-/-}$) compared with wildtype (wt) mice. In an RNA-sequencing approach of FACS sorted wt and HIF-2α$^{LysM-/-}$ TAMs, serine protease inhibitor, *Kunitz type-1* (*Spint1*) emerged as a promising candidate for HIF-2α-dependent regulation. We validated reduced *Spint1* messenger RNA expression and concomitant Spint1 protein secretion under hypoxia in HIF-2α-deficient bone marrow–derived macrophages (BMDMs) compared with wt BMDMs. In line with the physiological function of Spint1 as an inhibitor of hepatocyte growth factor (HGF) activation, supernatants of hypoxic HIF-2α knockout BMDMs, not containing Spint1, were able to release proliferative properties of inactive pro-HGF on breast tumor cells. In contrast, hypoxic wt BMDM supernatants containing abundant Spint1 amounts failed to do so. We propose that Spint1 contributes to the tumor-suppressive function of HIF-2α in TAMs in breast tumor development.

KEYWORDS
HAI-1, HGF, hypoxia, proliferation, tumor-associated macrophages

1 | INTRODUCTION

Breast cancer still accounts for most cancer-related deaths of women worldwide.[1] As in most solid cancers, hypoxia is an accompanying characteristic during cancer progression.[2] A lack of oxygen often results from a leaky and thus, inefficient tumor-associated vasculature.[3,4] Immune cell infiltrates and their metabolism augments oxygen shortage due to the adjustment of their activation status, differentiation, and cytokine-production profiles to either promote or suppress tumor growth. Upon tumor infiltration, monocytes differentiate into tumor-associated macrophages (TAMs), which accumulate in hypoxic areas, where they are educated to predominantly act tumor-supportive.[5-7] High numbers

Abbreviations: BMDM, bone marrow–derived macrophage; CCND1, cyclin D1; HGF, hepatocyte growth factor; HIF, hypoxia-inducible factor; LysMCre, lysozyme M Cre; PHD, prolyl hydroxylases; TAM, tumor-associated macrophage; wt, wildtype.

of TAMs are often associated with poor prognosis and chemoresistance in breast cancer.[8] Their protumor functions comprise the secretion of growth factors, stimulation of angiogenesis, and immunosuppression, while the secretion of proteolytic enzymes promotes tumor cell invasion and migration, and thus, supports metastasis. Several of these TAM-characteristic features are facilitated by hypoxia-inducible factors (HIFs).[9]

HIFs are heterodimeric transcription factors, sensing and coordinating cellular responses to hypoxia.[10,11] Their α-subunits (1α, 2α, or 3α) bind a common β-subunit (aryl hydrocarbon receptor nuclear translocator, [ARNT]) to induce a set of hypoxia-responsive genes. Both, α and β subunits belong to the PAS family of basic helix-loop-helix Per-ARNT-Sim proteins. While the β-subunit is constitutively expressed, the α-subunits are rapidly degraded under normoxic conditions. Specifically, prolyl hydroxylases (PHD) target the α-subunits for ubiquitin-dependent proteasomal degradation by hydroxylation of two conserved proline residues. As this process critically depends on oxygen as a cofactor, PHD enzymes are inactive under hypoxia. Upon stabilization, α-subunits dimerize with the β-subunit, followed by the translocation of the dimer to the nucleus and recognition of hypoxia-responsive elements to induce transcription of specific genes.[12,13] HIF-1α was identified first and found to be ubiquitously expressed in almost all cells. Classical HIF-1 target genes affect energy metabolism and glycolysis. The expression of HIF-2α, also known as endothelial PAS protein 1 (EPAS1), appears tissue-restricted, being highly abundant in endothelial and renal cells. HIF-2α target genes characterized so far mainly affect angiogenesis and erythropoiesis.[14] Of note, high expression of HIF-2α was also observed in macrophages suggesting a role in myeloid cell function.[15,16] As both α-subunits generate overlapping, but also distinct transcription profiles, their differential activities contribute to shape the versatile macrophage phenotypes specifically.[9,17,18]

The importance of myeloid HIF-1α for inflammatory and tumor-promoting properties of TAMs was pointed out by numerous studies. As myeloid HIF-1α is needed for adenosine triphosphate production, the energy-demanding processes of invasion and motility are severely impaired in TAMs lacking HIF-1α.[19,20] Attenuating proliferation and activity of tumor-infiltrating T cells appeared also to be HIF-1α-dependent, in part, by controlling the expression of L-arginine consuming enzymes such as inducible nitric oxide synthase (iNOS) and arginase 1 (Arg-1).[21,22] During inflammation HIF-1α is required for a full-blown bactericidal activity of macrophages, regulating the release of granule proteases and antimicrobial peptides.[23,24] In contrast, information on myeloid HIF-2α is limited, especially concerning its role in TAMs. Casazza et al[25] suggested HIF-2α to activate nuclear factor-κB (NF-κB) and to repress neuropilin 1 (Nrp1) to trap TAMs in hypoxic areas inside the tumor. Imtiyaz et al[26] analyzed macrophages during acute and tumor-associated inflammation and identified HIF-2α-dependent proinflammatory cytokine production. They further showed that the loss of myeloid HIF-2α reduced infiltration of TAMs into both murine hepatocellular and colitis-associated colon carcinoma models, attenuating tumor cell proliferation as well as tumor progression. Work from Roda and colleagues explored expression of HIF-2α and secretion of a soluble form of the vascular endothelial growth factor (VEGF) receptor (sVEGFR-1) in TAMs. sVEGFR-1 binds and neutralizes VEGF, which decreased vascularization of melanoma-bearing mice and reduced tumor growth.[27] It is also hypothesized that HIF-2α blocks the mitochondrial reactive oxygen species—*Marco* signaling axis to suppress the phagocytic activity of resting macrophages.[28]

Although the wealth of existing data suggests that both HIF isoforms are important for macrophage function, we still lack a complete picture to understand the overlapping vs distinct roles of each isoform for myeloid biology. To expand our understanding, especially of the role of HIF-2α in macrophages during tumor progression, we compared wildtype (wt) and myeloid HIF-2α knockout mice (HIF-2α$^{LysM-/-}$) in an allograft breast cancer model. Herein, we identified the serine protease inhibitor Spint1 (hepatocyte growth factor activator inhibitor type-1 [HAI-1]), as a novel HIF-2α target in macrophages. Furthermore, we observed that HIF-2α-dependent expression of Spint1 in TAMs limits tumor growth by suppressing the activation of hepatocyte growth factor (HGF).

2 | MATERIALS AND METHODS

2.1 | Materials

All chemicals were purchased from Sigma-Aldrich (Munich, Germany), if not indicated otherwise. Primers were ordered from biomers.net (Biomers, Ulm, Germany).

2.2 | Cell culture

The murine breast cancer cell line E0771 was purchased from ATCC-LGC Standards GmbH (Wesel, Germany) and cultured in RPMI 1640 supplemented with 10% heat-inactivated fetal calf serum (FCS), 100 U/mL penicillin, 100 µg/mL streptomycin, and 15 mM HEPES ([4-(2-hydroxyethyl)-1-piperazineethanesulfonic acid]; all from PAA Laboratories, Cölbe, Germany). Cells were cultured in a humidified atmosphere with 5% CO_2 at 37°C and were passaged when the density was approximately 90%. For RNA analysis, 5×10^5 E0771 cells were seeded 1 day before treatments in RPMI medium supplemented with 10% charcoal-stripped FCS (Thermo Fisher Scientific, Karlsruhe, Germany), 100 U/mL penicillin, 100 µg/mL streptomycin, and 15 mM HEPES. E0771 cells were incubated for 4 hours with 40 ng/mL Pro-HGF (R&D Systems, Wiesbaden, Germany), the c-Met inhibitor PF-04217903 (Merck, Darmstadt, Germany), recombinant mouse Spint1 (R&D Systems), and/or macrophage-conditioned medium (500 µL, description below).

Bone marrow–derived macrophages (BMDMs) were isolated from 10- to 12-week-old mice by flushing both tibias and femurs with phosphate-buffered saline (PBS). Cells were seeded in six-well plates and cultivated for 7 days in RPMI medium (10% FCS, 100 U/mL penicillin, 100 µg/mL streptomycin) supplemented with 20 ng/mL macrophage colony-stimulating factor ([M-CSF]; PeproTech, Hamburg, Germany) and 20 ng/mL granulocyte-macrophage colony-stimulating factor ([GM-CSF]; PeproTech). Medium was changed on day 3. BMDMs

were cultivated under normoxia (21% O_2) or hypoxia (1% O_2), followed by RNA extraction with 1 mL RLT buffer (RNeasy Micro Kit; Qiagen, Hilden, Germany). After 7 days, supernatants were collected and centrifuged (1000*g*, 5 minutes) for enzyme-linked immunosorbent assay (ELISA) measurements or to obtain macrophage-conditioned medium.

2.3 | Animals

Mice were housed in the central animal facility and kept under pathogen-free conditions. HIF-1$\alpha^{flox/flox}$/lysozyme M Cre ([LysMCre], HIF-1$\alpha^{LysM-/-}$) mice were obtained from Prof. R. S. Johnson. HIF-2$\alpha^{flox/flox}$/LysMCre (HIF-2$\alpha^{LysM-/-}$) mice were provided by Prof. M. C. Simon. The floxed sites flank exon 2 of the HIF-1α or HIF-2α genes, respectively. Mice with flanked loxP sites, which were negative for Cre recombinase, served as controls. For animal experiments, the guidelines of the Hessian animal care and use committee were followed.

2.4 | Breast cancer allograft model

About 5×10^4 murine E0771 breast adenocarcinoma cells were injected subcutaneously into breast glands 3 and 8 of 10- to 12-week-old female mice. Tumor size was measured every second day with calipers and calculated as follows: size = (length × width^2)/2. Mice were killed when the largest tumor reached 1.2 cm in diameter. Tumors were isolated for further experiments.

2.5 | Histology and immunohistochemistry

For metastases, lung tissue was fixed with 4% paraformaldehyde and embedded in paraffin. Then 4 µm slices were deparaffinized in xylene (Sigma-Aldrich, Steinheim, Germany) and stained with Mayer's hemalum (Merck). At least 10 independent sections of each lung were analyzed.

For tumor vascularization, tumor tissue was zinc-fixated and embedded in paraffin. For staining a catalyzed signal amplification (CSA) kit (Dako, Hamburg, Germany) was used. Anti-CD31 (Chemicon International, Temecula, CA) was incubated overnight at 4°C. Secondary antibody (biotinylated anti-rat [Dako]) was applied for 15 minutes. Positive signals were visualized using diaminobenzidine as a substrate for the peroxidase-coupled secondary antibody. Stained tissues were analyzed using an Axioskop 40 microscope (Zeiss, Jena, Germany). Quantification was done with HistoQuest 2.X (Tissue Gnostics, Wien, Austria).

2.6 | Flow cytometry

Flow cytometry was performed using an LSRII/Fortessa (BD Biosciences, Heidelberg, Germany) and data were evaluated with the FlowJo software V10 (Treestar, Ashland, OR). Tumors were dissociated using the tumor dissociation kit (Qiagen). BMDMs (isolated and differentiated as described above) were detached with Accutase (Merck). Single cell solutions were blocked with BD Fc Block Receptor Binding Inhibitor (BD eBioscience, Frankfurt, Germany) for 15 minutes on ice in the dark, followed by staining with fluorochrome-conjugated antibodies for 15 minutes on ice in the dark. Antibodies (all from BD eBioscience) were titrated for optimal concentration and compensated using CompBeads (BD eBioscience). The following antibodies were used for the detection of immune cell subsets in the tumors: anti-CD45-Vioblue, anti-CD11c-BV711, anti-CD11b-BV605, anti-CD49f-PE-CF594, anti-CD3-PE-CF594, anti-CD19-APC-H7, anti-CD90.2-PE, anti-F4/80-PE-Cy7, anti-Ly6C-PerCP-Cy5.5, anti-Ly6G-APC-Ly7, anti-MHC-II-APC, and anti-NK1.1-BV510 (for a detailed gating strategy see Figure S3). For the analysis of macrophage polarization the following antibodies were used: anti-CD80-PE and anti-CD206-FITC.

2.7 | Cytokine quantification

Frozen tumor tissue was pulverized using a mortar and resuspended in 2× PBS for 4 hours at 4°C. Cytokine concentrations were analyzed in tumor supernatants by flow cytometry (fluorescence-activated cell sorting [FACS]) using the mouse inflammation cytometric bead array ([CBA]; BD Biosciences). Samples were measured on a FACS Fortessa flow cytometer (BD Biosciences) and analyzed with the FCAP software (V1.0.1; BD Biosciences).

2.8 | RNA sequencing

Tumors from allograft mice were isolated and dissociated as described above. Single cell suspensions were blocked with Fc Block Receptor Binding Inhibitor (BD Biosciences) and stained with anti-CD45-Vioblue, anti-CD49f-PE-CF594, anti-CD115-PE, anti-Ly6G-APC, anti-Ly6C-PerCP-Cy5.5, and anti-F4/80-PE-Cy7 antibodies (all from BD Biosciences). TAMs were separated as CD45$^+$, Ly-6G$^-$, CD115$^+$, Ly-6C$^{low/-}$, and F4/80$^+$ cells using a FACS Aria sorter (BD Biosciences). RNA from TAMs was extracted using the RNeasy Micro Kit (Qiagen). RNA quality was evaluated on an Agilent 2100 Bioanalyzer using an RNA 6000 Pico Chip (Agilent Technologies, Santa Clara), followed by quantification with a Qubit HS RNA Assay Kit (Thermo Fisher Scientific). Ten nanograms of RNA was taken for library preparation using the SMARTer Stranded Total RNA-Seq Kit v2-Pico Input (Takara Bio, Frankfurt, Germany). Quantity and quality of the complementary DNA (cDNA) libraries were evaluated by Qubit ds DNA HS Assay Kit (Thermo Fisher Scientific) and Agilent DNA High Sensitivity DNA Chip (Agilent Technologies), respectively. The libraries were sequenced (single-end, 75 cycles) using the High Output Kit v2 on a NextSeq 500 sequencer (Illumina, San Diego). Quality of the sequencing reads was checked using FastQC (https://www.bioinformatics.babraham.ac.uk/projects/fastqc/). The reads were then trimmed using Trimmomatic[29] with following parameters: LEADING:5 TRAILING:5 SLIDINGWINDOW:4:15. The trimmed reads were mapped using STAR Aligner[30] and subsequently, features were generated using FeatureCount.[31] Differentially expressed genes were determined using the DESeq2 package[32] in R. The data that support the findings of this study are available from the corresponding author upon reasonable request. For the differentially expressed genes ($P < .05$, basemean >30) with an assigned canonical gene name the reads per kilobase million (RPKMs) of all samples were visualized in a heatmap using Morpheus (https://software.broadinstitute.org/morpheus). The

resulting candidates were screened for HIF-1α- and HIF-2α-binding sites using a previously published chromatin immunoprecipitation (ChIP)-seq data sets.[17] Binding sites residing within 250 kb of the respective genes were taken as indicator for a potential transcription regulatory-binding site.

2.9 | Enzyme-linked immunosorbent assay

Frozen tumor tissue was pulverized using a mortar and resuspended in 2× PBS (100 µL/50 µg tumor tissue) for 4 hours at 4°C. Supernatants (2 mL) of BMDMs were collected after differentiation under normoxia or hypoxia. Hundred microliter supernatant of BMDMs or tumor lysates was used to detect Spint1 by ELISA according to the protocol of the Mouse HAI-1 ELISA Kit (RayBiotech, GA).

2.10 | RNA isolation and quantitative polymerase chain reaction (qPCR)

RNA from BMDMs and sorted primary cells was extracted with the RNeasy Micro Kit (Qiagen), according to the manufacturer's protocol. RNA from E0771 cells was extracted using the peqGold RNAPure Kit (Peqlab, Erlangen, Germany) as described by the manufacturer. RNA was reverse-transcribed using the Maxima First-Strand cDNA Synthesis Kit (Thermo Fisher Scientific). qPCR was performed with the CFX96 Real-Time PCR Detection System and SYBR Green (both from Bio-Rad Laboratories, Munich, Germany). Primer sequences were: *iNOS*, sense 5′-ACC CTA AGA GTC ACA AAA TGG C-3′ and antisense 5′-TTG ATC CTC ACA TAC TGT GGA CG-3′; *tumor necrosis factor-α* [*TNF-α*], sense 5′-CCA TTC CTG AGT TCT GCA AAG G-3′ and antisense 5′-AGG TAG GAA GGC CTG AGA TCT TAT C-3′; *interleukin-1β* [*IL-1β*], sense 5′-AGG CCA CAG GTA TTT TGT CG-3′ and antisense 5′-GAC CTT CCA GGA TGA GGA CA-3′; *Arg-1*, sense 5′-GTG AAG AAC CCA CGG TCT GT-3′ and antisense 5′-CTG GTT GTC AGG GGA GTG TT-3′; *found in inflammatory zone 1* [*FIZZ1*], sense 5′-CCC TTC TCA TCT GCA TCT CC-3′ and antisense 5′-CAG TAG CAG TCA TCC CAG CA-3′; *transforming growth factor beta* [*TGF-β*], sense 5′-GGA CTC TCC ACC TGC AAG AC-3′ and antisense 5′-GAC TGG CGA GCC TTA GTT TG-3′; *Ki67*, sense 5′-ACC GTG GAG TAG TTT ATC TGG G-3′ and antisense 5′-TGT TTC CAG TCC GCT TAC TTC T-3′; *CyclinD1*, sense 5′-CAA CAG GTT GTA GGG CTG GT-3′ and antisense 5′-TTG TCC CCA ATC TCC TTG TC-3′; *Spint1*, sense 5′-GTC GGC GTA TGG CTC CTT T-3′ and antisense 5′-GCT TCG GTG TCC AGC ACA A-3′; *TATA-binding protein* [*TBP*], sense 5′-CTG ACC ACT GCA CCG TTG CCA-3′ and antisense 5′-GAC TGC AGC AAA TCG CTT GGG A-3′.

2.11 | Statistical analysis

Each experiment was performed at least three times and results are expressed as mean ± SEM. Statistical analyses were performed using the Student *t* test, the Wilcoxon signed-rank test or a two-way analysis of variance (ANOVA).

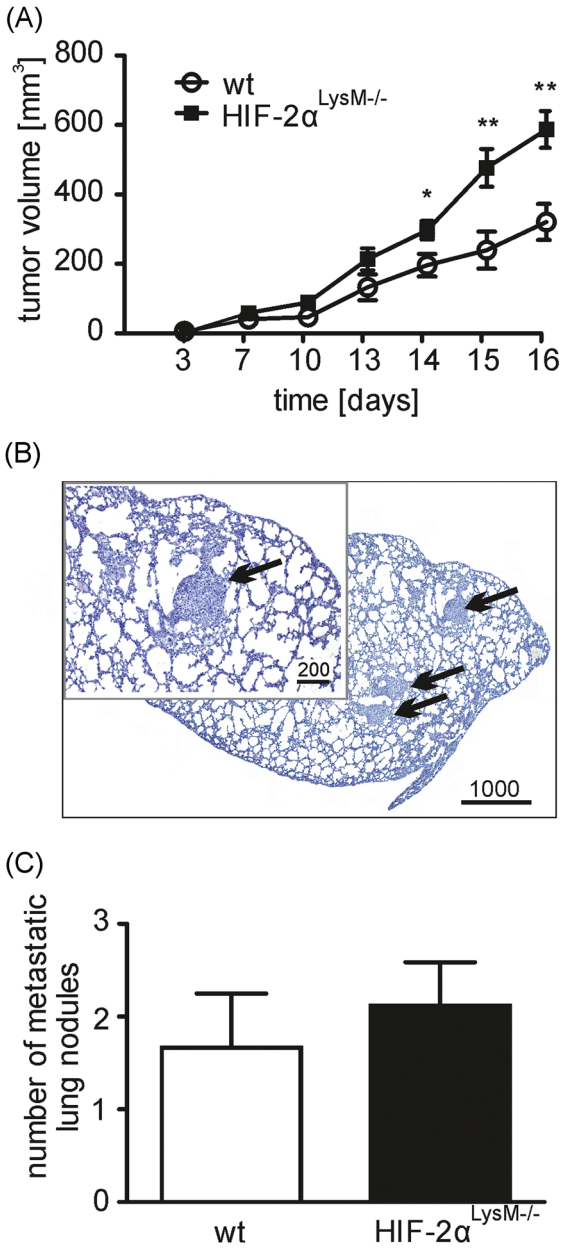

FIGURE 1 Effect of myeloid HIF-2α expression on breast tumor growth and metastasis. About 5×10^4 murine E0771 breast cancer cells were injected subcutaneously into breast glands 3 and 8 of 10- to 12-week-old female wt mice ($n = 10$) or HIF-2α$^{LysM-/-}$ mice ($n = 12$). A, Tumor size was determined every second day ($n = 20$ and 24 tumors for wt and HIF-2α$^{LysM-/-}$ mice, respectively). B, Representative lung sections from a HIF-2α$^{LysM-/-}$ mouse stained with Meyer's hemalum (scale bar = 1000 µm) and enlarged magnification (scale bar = 200 µm). Arrows indicate metastatic lung nodules. C, Number of metastatic lung nodules in wt and HIF-2α$^{LysM-/-}$ mice ($n = 10$ and 12 lungs for wt and HIF-2α$^{LysM-/-}$, respectively) killed when primary tumor size reached 1.2 cm. Data were analyzed using a two-way ANOVA with Bonferroni's correction (A) or a two-tailed Student *t* test (C) and represent mean ± SEM (*$P < .05$,**$P < .01$). ANOVA, analysis of variance; HIF, hypoxia-inducible factor; wt, wildtype [Color figure can be viewed at wileyonlinelibrary.com]

3 | RESULTS

3.1 | Deletion of HIF-2α in myeloid cells increases breast tumor growth

TAMs play a vital role during tumor development. While the role of macrophage HIF-1α is well documented, the function of HIF-2α in the context of TAMs is only poorly characterized, despite the fact that it appears to be expressed in macrophages.[15] To elucidate the impact of myeloid HIF-1α and HIF-2α in breast cancer development, mice with a myeloid-specific deletion of either HIF-1α or HIF-2α were generated using a Cre-Lox approach. The knockout was validated at RNA level in BMDMs from either HIF-1α$^{LysM-/-}$ or HIF-2α$^{LysM-/-}$ mice (Figure S1A and S1B). Subsequently, wt or HIF-1α$^{LysM-/-}$ or HIF-2α$^{LysM-/-}$ mice were subjected to an allograft breast cancer model. To this end, 5×10^4 E0771 breast cancer cells were injected subcutaneously into breast glands 3 and 8 of 12-week-old female wt, HIF-1α$^{LysM-/-}$, and HIF-2α$^{LysM-/-}$ mice. Three days after injection tumor nodules became palpable. Starting at day 14, tumors became significantly larger in HIF-2α$^{LysM-/-}$ mice compared with wt mice, reaching volumes of approximately 600 mm^3 and 300 mm^3 at day 16, respectively (Figure 1A). The maximally allowed tumor size of 1.2 cm was reached at least 2 days earlier in myeloid HIF-2α knockout mice compared with controls. In contrast, breast tumor development was comparable in HIF-1α$^{LysM-/-}$ and wt mice (Figure S2). As E0771 breast cancer cells have previously been shown to disseminate to the lungs, we next explored lung metastases in wt and HIF-2α$^{LysM-/-}$ mice. Histological evaluation of lungs from tumor-bearing mice revealed that lung nodules emerged in wt and HIF-2α$^{LysM-/-}$ mice at similar numbers (Figure 1B and 1C). Thus, myeloid HIF-2α attenuated tumor growth in an allograft breast cancer model but did not affect metastatic spread, whereas myeloid HIF-1α had no impact.

3.2 | Impact of myeloid HIF-2α on the breast tumor microenvironment

Taking the importance of the tumor microenvironment for the development of breast cancer into account, we aimed to characterize the role of myeloid HIF-2α. To this end, the immune cell composition

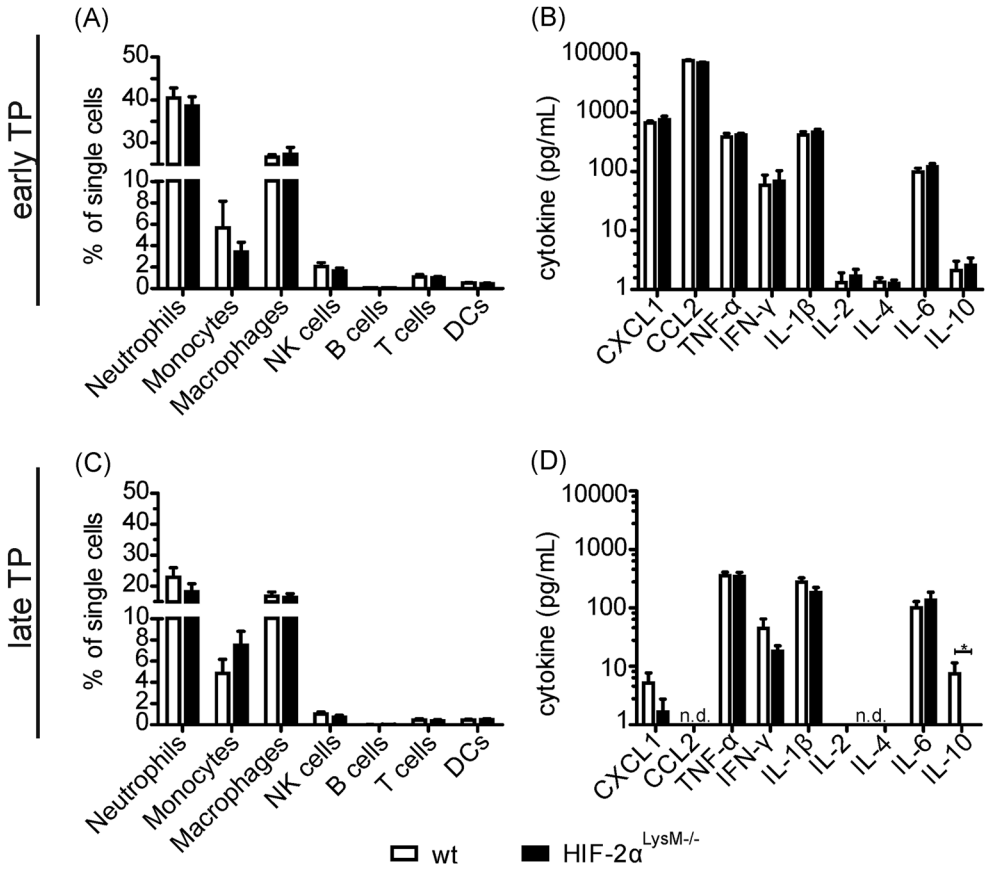

FIGURE 2 Effect of myeloid HIF-2α on the immune cell-shaped tumor microenvironment. Immune cell infiltration and cytokine production were analyzed in tumors isolated at the same day (day 14) (A and B; early time point [TP]) or when tumors reached the same tumor size (1.2 cm) (C and D; late TP) from wt or HIF-2α$^{LysM-/-}$ mice. A and C, Immune cell subsets from dissociated tumors were measured by polychromatic flow cytometry. The gating strategy is depicted in Figure S3. B and D, Cytokine levels in tumor lysates were quantified by cytometric bead arrays. Data were analyzed using a two-way ANOVA with Bonferroni's correction and represent mean ± SEM ($n \geq 4$, $^*P < .05$). ANOVA, analysis of variance; CCL2, C-C motif ligand 2; CXCL 1, C-X-C motif ligand 1; DC, dendritic cell; HIF, hypoxia-inducible factor; IFN, interferon; IL, interleukin; NK, natural killer; TNF, tumor necrosis factor

and the cytokine levels of tumors were analyzed by polychromatic flow cytometry (for gating strategy see Figure S3) in tumors from wt and HIF-2α$^{LysM-/-}$ mice isolated either following an equal growth period (ie, at day 14, early time point [TP]), or when tumors reached the predefined endpoint size (1.2 cm), referred to as the late TP. Surprisingly, neither myeloid-derived (neutrophils, monocytes, macrophages, dendritic cells) nor lymphoid cell subtypes (NK [natural killer] cells, B cells, T cells) displayed differences when comparing wt and myeloid HIF-2α knockout tumors at early or late TP (Figure 2A and 2C). However, markedly more neutrophils and, to a lesser degree, also more macrophages were present at early TP as compared with late TP, irrespective of the genetic background. Similarly, soluble mediators that typically shape the tumor microenvironment, including C-X-C motif ligand 1 (CXCL1), C-C motif ligand 2 (CCL2), TNF-α, interferon-γ (IFN-γ), interleukin (IL)−1β, IL-2, IL-4, and IL-6, remained unaltered between wt and myeloid HIF-2α knockout tumors at both TP (Figure 2B and 2D). In line with the reduced presence of neutrophils and macrophages, the respective chemoattractant CXCL1[33] and CCL2[34] were strongly reduced at later TP. IL-10 was the only cytokine that was reduced in tumors from HIF-2α$^{LysM-/-}$ mice as compared with wt mice, but only at late TP.

As IL-10 is associated with an alternative macrophage phenotype, we next asked whether myeloid HIF-2α might affect tumor growth by altering polarization of macrophages. To this end, we compared polarization markers in BMDMs of wt or HIF-2α$^{LysM-/-}$ mice. Surface expression of the polarization markers CD80 and CD206, representing established classical vs alternative markers, were similar in wt and myeloid HIF-2α knockout BMDMs (Figure 3A). Moreover, messenger RNA (mRNA) expression of additional classical (*IL-1β*, *iNOS*, *TNF-α*) and alternative markers (*Arg-1*, *TGF-β*, and *FIZZ1*) remained unaltered (Figure 3B). Furthermore, myeloid depletion of HIF-2α did not affect polarization of TAMs infiltrated in the breast cancer allograft model, as assessed by staining of macrophage polarization markers iNOS and Ym1 (chitinase-like 3) in tumor sections (Figure 3C). Interestingly, despite the enhanced tumor growth in HIF-2α$^{LysM-/-}$ mice, tumor vascularization, as measured by the number of CD31-positive cells in tumor sections, also did not vary compared with wt mice (Figure 3C). Taken together, myeloid HIF-2α-dependent changes in tumor growth unexpectedly occurred independently of immune cell infiltration and polarization.

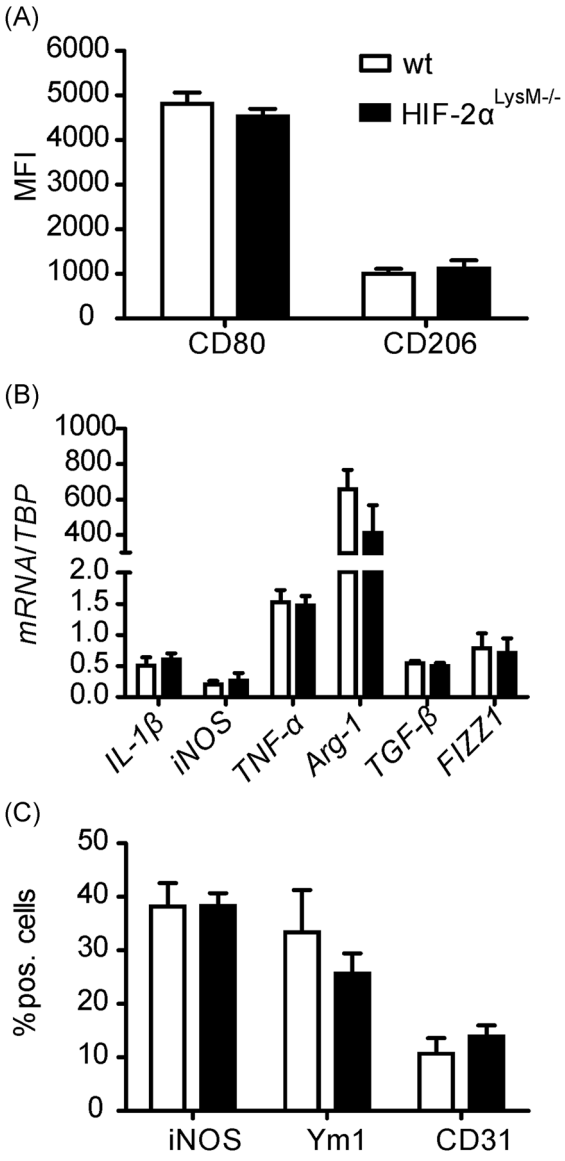

FIGURE 3 Effect of myeloid HIF-2α on macrophage polarization. A, Surface expression of polarization markers on wt or HIF-2α$^{LysM-/-}$ BMDMs was determined by FACS analysis and is depicted as mean fluorescence intensity (MFI). B, mRNA expression of polarization markers of wt or HIF-2α$^{LysM-/-}$ BMDMs was analyzed by qPCR and is given relative to *TBP*. C, Relative number of iNOS, Ym1, and CD31-positive cells in tumors isolated from wt or HIF-2α$^{LysM-/-}$ mice was determined by immunohistochemistry. Data were analyzed using a two-way ANOVA with Bonferroni's correction and represent mean ± SEM ($n \geq 4$). ANOVA, analysis of variance; Arg, arginase; BMDM, bone marrow–derived macrophage; FACS, fluorescence-activated cell sorting; FIZZ, found in inflammatory zone; HIF, hypoxia-inducible factor; IL, interleukin; iNOS, inducible nitric oxide synthase; mRNA, messenger RNA; TBP, TATA-binding protein; TGF, transforming growth factor; TNF, tumor necrosis factor

3.3 | HIF-2α-dependent gene expression changes in TAMs

As immune responses did not contribute to enhanced tumor growth in myeloid HIF-2α knockout mice, we determined HIF-2α-dependent differences in gene expression of TAMs. To allow for cell type-specific gene expression profiling, we isolated TAMs from tumors with a size of 1.2 cm by FACS using the gating strategy depicted in Figure S4. Specifically, within the immune cells (CD45$^+$) TAMs were defined as CD45$^+$, Ly-6G$^-$, CD115$^+$, Ly-6C$^{low/-}$, and F4/80$^+$. RNA-seq analysis of isolated TAMs identified 360 mRNAs with a more than 2-fold change (log2FC > 1 or log2FC < −1) in expression ($P \leq .05$) between wt and HIF-2α knockout macrophages. Amongst the confidentially described candidates, 83 showed appreciable expression across all samples (basemean > 30) (Figure 4A). While HIF-2α functions as a transcription factor facilitating adaptations to hypoxia,

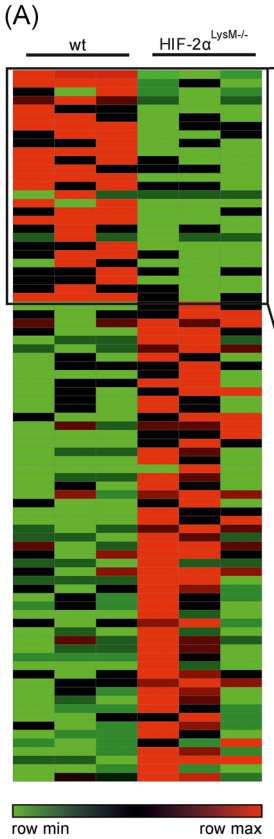

(B)

Gene	log2 (FC)	p value	Binding site (1α/2α)
Lyz2	-7.047292	1.22E-87	No
Gdf3	-3.129569	5.43E-09	1α and 2α
Spint1	-2.569340	0.030993	2α
Gatm	-1.939698	4.84E-10	1α and 2α
Plxnd1	-1.444073	3.09E-09	No
Tmem26	-1.307279	0.000342	No
Tmem86a	-1.291697	0.000352	No
Apobec1	-1.275333	8.70E-08	1α and 2α
Il10	-1.267676	0.001699	2α
Ttc38	-1.258827	0.012180	No
Cdc42ep3	-1.237903	0.000243	No
B3galt6	-1.220606	0.020488	1α and 2α
Cnksr3	-1.212361	0.010907	1α and 2α
Cbr2	-1.203504	0.015443	No
Cadm1	-1.200729	0.029734	No
Rpusd1	-1.192426	0.025078	1α
Apoe	-1.166488	0.000751	1α
Tgfbr2	-1.153846	2.63E-07	1α and 2α
Slc13a3	-1.147590	0.001028	No
Astl	-1.140259	0.030695	No
Depdc7	-1.099912	0.004064	2α
Zfp74	-1.085555	0.023571	No
Pou2f2	-1.067061	0.010177	No
Selenop	-1.056825	0.000599	No
Guk1	-1.047044	0.007526	1α
Zfp422	-1.035361	0.028020	No
Siglec1	-1.007014	0.000115	No

FIGURE 4 Differential gene expression of wt vs HIF-2α knockout TAMs. RNA expression was determined in TAMs from tumors isolated from wt or HIF-2α$^{LysM-/-}$ mice by RNA-seq analysis. A, Heatmap of the top 83 differentially expressed genes between wt and HIF-2α knockout TAMs (columns represent individual mice; $n = 3$). B, List of genes with significantly reduced expression in HIF-2α knockout as compared with wt TAMs (log2 fold change [log2FC], *P* value, predicted HIF-1α-/HIF-2α-binding sites). HIF, hypoxia-inducible factor; TAM, tumor-associated macrophage; wt, wildtype [Color figure can be viewed at wileyonlinelibrary.com]

only 32.9% (27 mRNAs) of the differentially expressed genes were reduced in HIF-2α-deficient TAMs (Figure 4B). Nevertheless, the knockout status was confirmed by the massively reduced expression of *lysozyme 2* (*Lyz2*) mRNA in knockout cells, confirming the Cre recombinase insertion. Focusing on those mRNAs that appeared to be transcriptionally dependent on HIF-2α and given our interest in targets exclusively regulated by HIF-2α, we used recently published ChIP-seq data,[17] checking for both HIF-1α- and HIF-2α-binding sites within the gene loci of the identified targets or in the vicinity thereof, that is within 250 kb of the target genes. While the majority of predicted targets either contained no HIF-binding sites (55.5%) or binding sites for both HIF isoforms (22.2%), only three candidates (*Spint1*, *IL-10*, *Depdc7*) appeared as exclusive HIF-2 targets (Figure 4B). Amongst the transcriptionally regulated HIF-2-specific candidates, *Spint1* displayed the strongest reduction in HIF-2α knockout TAMs (log2FC = −2.57). As Spint1 was previously shown to inhibit cancer progression,[35] it emerged as an interesting candidate that might be involved in the tumor-suppressive function of myeloid HIF-2α.

To confirm Spint1 as a myeloid HIF-2α target, BMDMs were isolated from wt and HIF-2α$^{LysM-/-}$ mice, differentiated to macrophages with M-CSF and GM-CSF for 7 days, either under hypoxic (1%) or normoxic (21%) conditions before mRNA expression analysis of *Spint1*. mRNA expression of *Spint1* was markedly lower in HIF-2α$^{LysM-/-}$ BMDMs compared with wt BMDMs under normoxic conditions. Furthermore, *Spint1* mRNA expression significantly increased in wt BMDMs during prolonged periods of hypoxia, whereas it was not hypoxia responsive in HIF-2α$^{LysM-/-}$ BMDMs (Figure 5A). To assess if transcriptional changes observed for *Spint1* are also reflected at protein level, we next analyzed Spint1 protein by ELISA in the supernatants of BMDMs. In line with the changes at mRNA level, Spint1 protein increased under hypoxia in the supernatants of wt BMDMs, whereas it remained low, under normoxia and hypoxia in HIF-2α$^{LysM-/-}$ BMDM supernatants (Figure 5B). Since Spint1 occurs in a secreted as well as in a membrane-bound form, we evaluated Spint1 protein in BMDM lysates as well. Spint1 was present at much higher levels in lysates of wt as compared with HIF-2α-deficient BMDMs. In contrast to the extracellular protein and the mRNA expression, cellular Spint1 protein did not increase in response to hypoxia (Figure S5). Reduced viability of HIF-2α knockout BMDMs under hypoxic conditions was further excluded as a contributing factor using caspase-3 activity assays (Figure S6).

To assess whether reduced Spint1 expression in HIF-2α knockout TAMs (Figure 4B) and BMDMs (Figure 5A and 5B) altered Spint1 levels also in whole tumors, we analyzed *Spint1* mRNA expression in tumors of wt and HIF-2α$^{LysM-/-}$ mice isolated either at day 14 (early

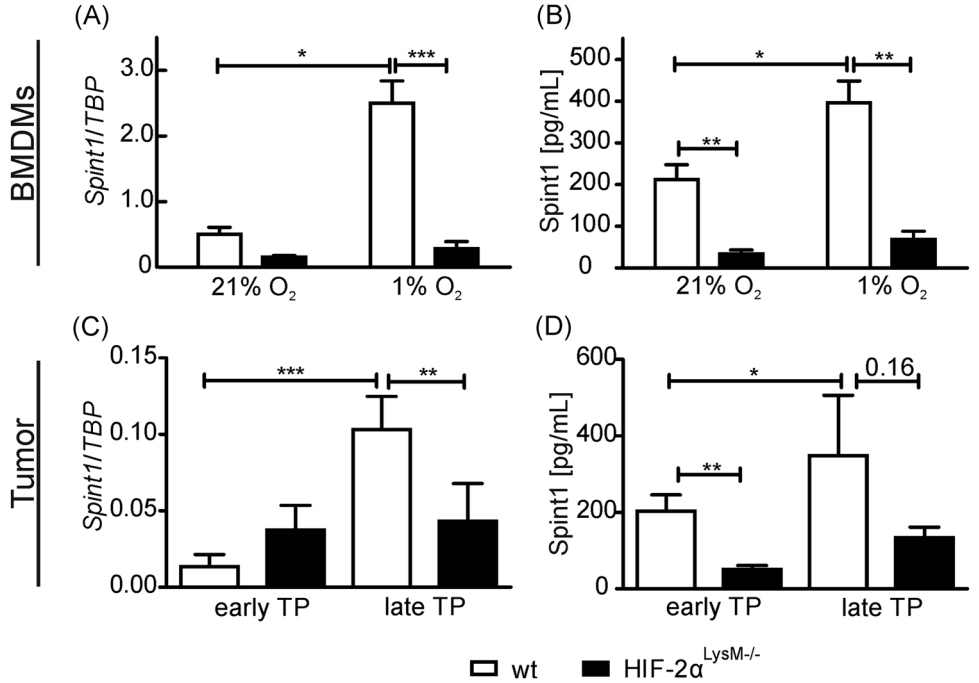

FIGURE 5 Expression of Spint1 in wt vs HIF-2α knockout macrophages and associated tumors. A and B, wt and HIF-2α$^{LysM-/-}$ BMDMs were incubated for 7 days under 21% or 1% O_2, before (A) *Spint1* mRNA expression was analyzed by qPCR and is given relative to *TBP*, or (B) Spint1 protein was determined in the BMDM supernatants by ELISA. C and D, Spint1 was analyzed in tumors isolated at the same day (day 14; early TP) or when they reached the same tumor size (1.2 cm) (late TP) from wt and HIF-2α$^{LysM-/-}$ tumors. C, *Spint1* mRNA expression was analyzed by qPCR and is given relative to *TBP*. D, Spint1 protein levels in tumor lysates were quantified by ELISA. Data were analyzed using a two-way ANOVA with Bonferroni's correction and represent mean ± SEM ($n \geq 3$, $^{*}P < .05$, $^{**}P < .01$ $^{***}P < .001$). ANOVA, analysis of variance; BMDM, bone marrow–derived macrophage; ELISA, enzyme-linked immunosorbent assay; HIF, hypoxia-inducible factor; qPCR, quantitative polymerase chain reaction; TBP, TATA-binding protein; TP, time point; wt, wildtype

TP) or when an equal tumor size of 1.2 cm was reached (late TP). *Spint1* expression increased in tumors growing in wt mice, comparing early vs late tumor growth. In contrast, *Spint1* levels remained unaltered in tumors of myeloid HIF-2α knockout mice (Figure 5C). Interestingly, while Spint1 protein also increased in tumor lysates of wt mice during tumor progression, it was markedly reduced at both TP in tumors of HIF-2α$^{LysM-/-}$ as compared with wt mice (Figure 5D). Our experiments therefore establish Spint1 as a novel hypoxia-responsive HIF-2α target in macrophages.

3.4 | HIF-2α-dependent expression of Spint1 is tumor suppressive

Spint1 is characterized as an inhibitor of the serine protease HGF activator (HGFA), which is critically required for activation of HGF, which enhances tumor cell proliferation.[36] Considering the lower levels of Spint1 in the supernatants of HIF-2α knockout BMDMs, we asked if activation of HGF might contribute to the enhanced tumor growth in HIF-2α$^{LysM-/-}$ mice. We first analyzed expression of the proliferation markers cyclin D1 (CCND1) and Ki67 in E0771 tumor cells treated with the supernatants of either wt or HIF-2α$^{LysM-/-}$ BMDMs. Yet, neither wt nor HIF-2α knockout supernatants induced *CCND1* or *Ki67* expression in comparison to untreated E0771 cells (Figure 6A and 6B). To assess, if the availability of activatable pro-HGF might have been limiting in this experimental setting, we supplemented either control medium or BMDM supernatants with recombinant pro-HGF. Supplementation of pro-HGF in control medium did not affect expression of the proliferation markers (Figure 6C and 6D), indicating that pro-HGF did not get activated under these circumstances, despite the presence of FCS in the medium. Interestingly, while *HGFA* mRNA expression appeared to be extremely low in E0771 cells, it was highly abundant in hypoxic BMDMs from wt and HIF-2α$^{LysM-/-}$ mice. In contrast, while HGFA protein expression in BMDMs was confirmed by Western blot analysis, it was much higher in E0771 tumor cells (Figure S7). In line with the finding that HIF-2α-deficient BMDMs do not secrete appreciable amounts of Spint1, the addition of pro-HGF induced expression of the proliferation markers *CCND1* and *Ki67* only in E0771 cells incubated with supernatants of HIF-2α knockout BMDMs, while Spint1-containing supernatants of wt BMDMs did not enhance proliferation, even when pro-HGF was added (Figure 6C and 6D). To gain further evidence for the importance of the HGF-activating function of HIF-2α BMDM supernatants, we next aimed to overcome the proliferative properties of pro-HGF supplemented HIF-2α BMDM supernatants by adding either recombinant Spint1 or an inhibitor for the HGF receptor c-Met (PF-04217903). Indeed, both Spint1 and PF-04217903 reduced *CCND1* and *Ki67* expression to control levels (Figure 6E and 6F). In summary, our data suggest that

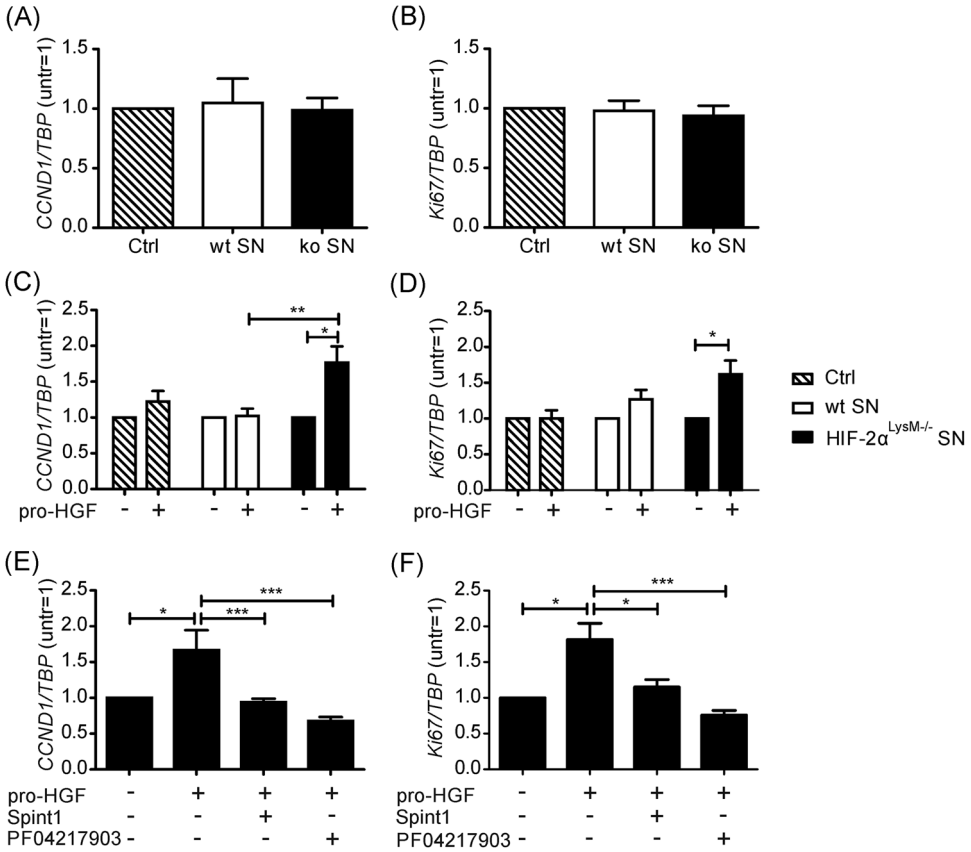

FIGURE 6 Effect of supernatants from wt or HIF-2α knockout macrophages on tumor cell proliferation. A and B, Proliferation markers were analyzed in E0771 cells treated with supernatants from hypoxic wt or HIF-2α knockout BMDMs and normalized to untreated controls ($n = 12$). C and D, Proliferation markers were analyzed in E0771 cells treated with BMDM supernatants or control medium supplemented with pro-HGF (40 ng/mL) and normalized to the respective nonsupplemented samples ($n = 8$). E and F, Proliferation markers were analyzed in E0771 cells treated with supernatants from HIF-2α knockout BMDMs supplemented with pro-HGF (40 ng/mL) in combination with recombinant Spint1 (100 ng/mL) or the c-Met inhibitor PF-04217903 (250 nM) and normalized to the nonsupplemented sample ($n = 8$). mRNA expression of the proliferation markers *CCND1* (A, C, E) and *Ki67* (B, D, F) were analyzed by qPCR and is given relative to *TBP*. SN = supernatant; untr = untreated. Data were analyzed using the Wilcoxon signed-rank test (A, B, C, D, E, F) or a two-tailed Student *t* test (C, D) and represent mean ± SEM (*$P < .05$, **$P < .01$, ***$P < .001$). BMDM, bone marrow–derived macrophage; CCND1, cyclin D1; Ctrl, control; HGF, hepatocyte growth factor; mRNA, messenger RNA; qPCR, quantitative polymerase chain reaction; SN, supernatant; TBP, TATA-binding protein; untr, untreated; wt, wildtype

HIF-2α-dependent expression of Spint1 in TAMs inhibits the activation of the growth factor HGF and proliferation of tumor cell.

4 | DISCUSSION

In the present study, we provide evidence for a tumor-suppressive function of HIF-2α in TAMs. We observed that HIF-2α is strongly expressed in primary murine macrophages cultured under hypoxic conditions in vitro. Of note, HIF-2α expression in macrophages is required to induce the production of the serine protease inhibitor Spint1, which inhibits activation of the proliferative growth factor HGF and thus, limits tumor growth. Consequently, the HIF-2α–Spint1 axis emerges as a so far uncharacterized tumor-suppressive entity in murine breast tumor development (Figure 7).

In contrast to HIF-1α, HIF-2α, the regulated subunit of the HIF-2 transcription factor, is expressed only in specific tissue types. Appreciable HIF-2α expression was previously shown for endothelial cells, renal cells, and within the immune cell compartment, only in macrophages.[37-39] Specifically, HIF-2α appeared to be selectively expressed in TAMs in various tumor types,[15] yet its exact role in the tumor context remains controversially discussed. While high HIF-2α expression in TAMs of invasive breast carcinoma patients was correlated with enhanced tumor vascularization and grade,[40] we previously found accelerated tumor growth upon depletion of myeloid HIF-2α in a 3-methylcholanthrene (MCA)-induced fibrosarcoma mouse model.[41] Similarly, a HIF-2α knockout in myeloid cells enhanced growth of E0771 breast tumor allografts in the present study. Of note, in contrast to previous findings that myeloid HIF-1α depletion reduced tumor growth in the polyoma middle T (PyMT)-driven breast cancer model[21] as well as in the MCA-induced fibrosarcoma model,[41] E0771 allograft growth was not affected by a myeloid HIF-1α knockout, suggesting a highly tumor-specific role of myeloid HIF-1α. In line with enhanced tumor growth in myeloid HIF-2α-depleted mice in our model, an antitumor function of myeloid HIF-2α was demonstrated in xenograft mouse models of malignant

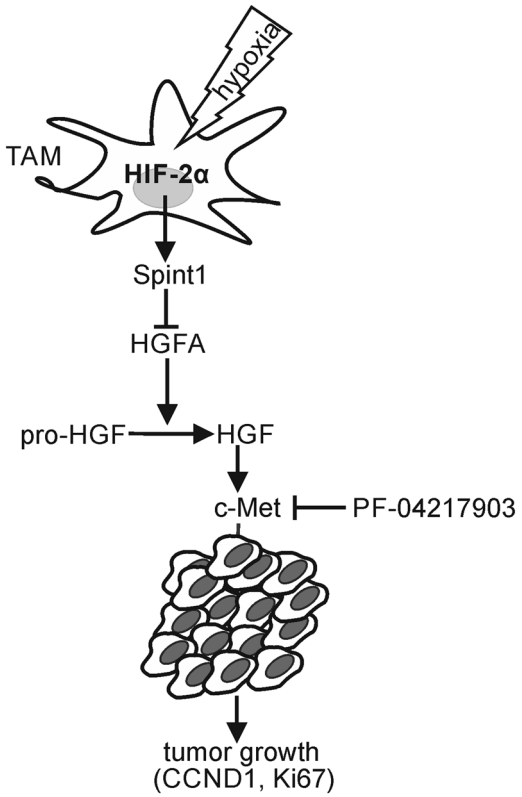

FIGURE 7 Proposed model for the role of HIF-2α in TAMs on tumor growth. HIF-2α induces the expression of Spint1 in TAMs in response to hypoxia. Spint1 is released into the tumor microenvironment, where it inhibits the serine protease HGFA, thereby preventing pro-HGF cleavage into active HGF. If HGF cannot bind to its receptor c-Met on tumor cells, tumor cell proliferation is reduced. CCND1, cyclin D1; HGFA, HGF activator; HIF, hypoxia-inducible factor; TAM, tumor-associated macrophage

melanomas, where HIF-2α-dependent production of the soluble form of the VEGF receptor (sVEGFR-1) by macrophages reduced tumor growth and vascularization.[27,42] The observation that elevated HIF-2α expression enhanced tumor cell apoptosis and reduced tumor vascularization in a rat glioma model further supported antitumor properties of HIF-2α.[43] Whereas our data also support a tumor-suppressive role of myeloid HIF-2α, it neither appeared to depend on differences in tumor vascularization nor on changes in immune cell infiltration, as previously suggested for hepatocellular and colitis-associated colon carcinoma mouse models.[26] Furthermore, while myeloid HIF-2α was previously shown to be essential for an alternative macrophage phenotype in thioglycollate-elicited peritoneal macrophages,[44] macrophage polarization was not altered in HIF-2α knockout macrophages (BMDMs and TAMs) in our study. In contrast, our data suggest that the newly identified HIF-2α target Spint1 contributes to reduced tumor cell proliferation. Spint1 is well characterized to inhibit HGF-dependent cell proliferation and consequently attenuates tumor growth.[35,45] Specifically, Spint1 inhibits HGFA, which is required in the extracellular space to activate pro-HGF. Activated HGF exerts its effects on target cells by binding to and activating its receptor c-Met.[46] Activation of c-Met, in turn, enhances proliferation, cell survival, organ morphogenesis, neovascularization, tissue repair, and regeneration.[47] In fact, enhanced expression of *CCND1* and *Ki67* in tumor cells within a macrophage-shaped environment was sensitive to both elevated Spint1 levels and the c-Met inhibitor PF-04217903, supporting a proliferation-supportive function of the HGF/c-Met axis in our experimental setting. Interestingly, active c-Met signaling was also suggested to affect invasive and metastatic properties of tumors instead of enhancing their proliferation.[48] Our observation that HIF-2α-dependent elevation of Spint1 contributed to reduced tumor cell proliferation in vitro and correlated with attenuated tumor growth in vivo, corroborates previous reports, proposing that aberrant c-Met activation by HGF enhanced tumor growth and correlated with poor prognosis,[46,47] yet, the value of c-Met expression as a prognostic marker appears limited.[49] Nevertheless, c-Met was even put forward as a promising candidate for tumor therapeutic interventions.[50-53] Importantly, our findings extend the current model of HGF-dependent, c-Met-mediated tumor growth, to include TAMs as an important source of the inhibitory Spint1. We further provide evidence for a HIF-2α-dependent Spint1 production in TAMs. The observation that Spint1 protein levels increased in the supernatants (ie, soluble form) but not in the cell lysates (ie, membrane-bound form) of wt BMDMs in response to hypoxia, suggests that either shedding of Spint1 might not be limiting under these experimental conditions or that hypoxia not only enhances production but also shedding of Spint1. As a side note, while our experiments corroborate earlier findings that tumor cells are an important source of HGFA in the tumor context,[54,55] we found evidence that TAMs also produce HGFA protein and even express much higher levels of HGFA mRNA than tumor cells. Yet, further studies are needed to determine the impact of TAM-derived HGFA in tumors. In contrast, pro-HGF within the tumor microenvironment likely stems from other sources than tumor cells and macrophages. While there is abundant evidence that cancer-associated fibroblasts are a major source of pro-HGF in breast carcinomas,[46,56-58] adipocytes derived from monocyte/macrophage progenitors were recently shown to provide HGF to enhance migration of tumor cells when coinjected subcutaneously with E0771 cells into mice.[59]

Interestingly, while we found many genes to be differentially expressed between wt and HIF-2α knockout TAMs, only roughly a third showed reduced expression in HIF-2α-deficient macrophages, indicative for a potential direct transcriptional regulation. Moreover, only a small fraction of these emerged as HIF-2-exclusive candidates. Thus, it will be interesting to see, if the differentially expressed genes lacking a previously identified HIF-binding site might share characteristics that allow for parallel HIF-2α-dependent regulation.

In summary, our study supports a novel tumor-suppressive function of HIF-2α in TAMs in breast tumors. In detail, HIF-2α-dependent regulation of the HGF-activation inhibitor Spint1 limited tumor cell proliferation, thereby reducing tumor growth. Our findings not only provide new insights into the role of HIF-2α in tumor development but also add another facet to the impact of

TAMs on tumor progression in general. These data indicate that macrophages in the tumor context not only exert protumorigenic functions, yet still might retain some of their tumor-suppressive properties. This underscores the importance to consider all aspects of the complex interplay of tumors with their microenvironment for the development of future, molecularly targeted therapeutic approaches.

ACKNOWLEDGMENTS

We thank Bettina Wenzel and Tanja Keppler for excellent technical assistance. Grant support: DFG:SFB815—project A8 (to BB).

ORCID

Tobias Schmid http://orcid.org/0000-0002-1952-5259
Bernhard Brüne http://orcid.org/0000-0001-8237-2841

REFERENCES

1. Siegel RL, Miller KD, Jemal A. Cancer statistics, 2017. *CA Cancer J Clin*. 2017;67(1):7-30.
2. Semenza GL. Defining the role of hypoxia-inducible factor 1 in cancer biology and therapeutics. *Oncogene*. 2010;29(5):625-634.
3. Huang D, Li C, Zhang H. Hypoxia and cancer cell metabolism. *Acta Biochim Biophys Sin*. 2014;46(3):214-219.
4. Eales KL, Hollinshead KER, Tennant DA. Hypoxia and metabolic adaptation of cancer cells. *Oncogenesis*. 2016;5:e190.
5. Murdoch C, Muthana M, Lewis CE. Hypoxia regulates macrophage functions in inflammation. *J Immunol*. 2005;175(10):6257-6263.
6. Schreiber RD, Old LJ, Smyth MJ. Cancer immunoediting: integrating immunity's roles in cancer suppression and promotion. *Science*. 2011; 331(6024):1565-1570.
7. Palazón A, Aragonés J, Morales-Kastresana A, De Landázuri MO, Melero I. Molecular pathways: hypoxia response in immune cells fighting or promoting cancer. *Clin Cancer Res*. 2012;18(5):1207-1213.
8. Qiu S-Q, Waaijer SJH, Zwager MC, de Vries EGE, van der Vegt B, Schröder CP. Tumor-associated macrophages in breast cancer: innocent bystander or important player? *Cancer Treat Rev*. 2018; 70:178-189.
9. Henze AT, Mazzone M. The impact of hypoxia on tumor-associated macrophages. *J Clin Invest*. 2016;126(10):3672-3679.
10. Pugh CW, O'Rourke JF, Nagao M, Gleadle JM, Ratcliffe PJ. Activation of hypoxia-inducible factor-1; definition of regulatory domains within the α subunit. *J Biol Chem*. 1997;272(17):11205-11214.
11. Huang LE, Gu J, Schau M, Bunn HF. Regulation of hypoxia-inducible factor 1 is mediated by an O_2-dependent degradation domain via the ubiquitin-proteasome pathway. *Proc Natl Acad Sci USA*. 1998;95(14): 7987-7992.
12. Koh MY, Powis G. Passing the baton: the HIF switch. *Trends Biochem Sci*. 2012;37(9):364-372.
13. Wu D, Potluri N, Lu J, Kim Y, Rastinejad F. Structural integration in hypoxia-inducible factors. *Nature*. 2015;524(7565):303-308.
14. Keith B, Johnson RS, Simon MC. HIF1α and HIF2α: sibling rivalry in hypoxic tumour growth and progression. *Nat Rev Cancer*. 2012;12(1):9-22.
15. Talks KL, Turley H, Gatter KC, et al. The expression and distribution of the hypoxia-inducible factors HIF-1α and HIF-2α in normal human tissues, cancers, and tumor-associated macrophages. *Am J Pathol*. 2000;157(2):411-421.
16. Griffiths L, Binley K, Iqball S, et al. The macrophage—a novel system to deliver gene therapy to pathological hypoxia. *Gene Therapy*. 2000; 7(3):255-262.
17. Tausendschön M, Rehli M, Dehne N, et al. Genome-wide identification of hypoxia-inducible factor-1 and -2 binding sites in hypoxic human macrophages alternatively activated by IL-10. *Biochim Biophys Acta Gene Regul Mech*. 2015;1849(1):10-22.
18. Fang H-Y, Hughes R, Murdoch C, et al. Hypoxia-inducible factors 1 and 2 are important transcriptional effectors in primary macrophages experiencing hypoxia. *Blood*. 2009;114(4):844-859.
19. Lin N, Simon MC. Hypoxia-inducible factors: key regulators of myeloid cells during inflammation. *J Clin Invest*. 2016;126(10):3661-3671.
20. Cramer T, Yamanishi Y, Clausen BE, et al. HIF-1α is essential for myeloid cell-mediated inflammation. *Cell*. 2003;112(5):645-657.
21. Doedens AL, Stockmann C, Rubinstein MP, et al. Macrophage expression of hypoxia-inducible factor-1 suppresses T-cell function and promotes tumor progression. *Cancer Res*. 2010;70(19):7465-7475.
22. Thiel M, Caldwell CC, Kreth S, et al. Targeted deletion of HIF-1α gene in T cells prevents their inhibition in hypoxic inflamed tissues and improves septic mice survival. *PLoS One*. 2007;2(9):e853.
23. Peyssonnaux C, Datta V, Cramer T, et al. HIF-1α expression regulates the bactericidal capacity of phagocytes. *J Clin Invest*. 2005;115(7): 1806-1815.
24. Anand RJ, Gribar SC, Li J, et al. Hypoxia causes an increase in phagocytosis by macrophages in a HIF-1α-dependent manner. *J Leukoc Biol*. 2007;82(5):1257-1265.
25. Casazza A, Laoui D, Wenes M, et al. Impeding macrophage entry into hypoxic tumor areas by Sema3A/Nrp1 signaling blockade inhibits angiogenesis and restores antitumor immunity. *Cancer Cell*. 2013; 24(6):695-709.
26. Imtiyaz HZ, Williams EP, Hickey MM, et al. Hypoxia-inducible factor 2α regulates macrophage function in mouse models of acute and tumor inflammation. *J Clin Invest*. 2010;120(8):2699-2714.
27. Roda JM, Wang Y, Sumner LA, Phillips GS, Marsh CB, Eubank TD. Stabilization of HIF-2α induces sVEGFR-1 production from tumor-associated macrophages and decreases tumor growth in a murine melanoma model. *J Immunol*. 2012;189(6):3168-3177.
28. Dehn S, Deberge M, Yeap X-Y, et al. HIF-2α in resting macrophages tempers mitochondrial reactive oxygen species to selectively repress MARCO-dependent phagocytosis. *J Immunol*. 2016;197(9):3639-3649.
29. Bolger AM, Lohse M, Usadel B. Trimmomatic: a flexible trimmer for Illumina sequence data. *Bioinformatics*. 2014;30(15):2114-2120.
30. Dobin A, Davis CA, Schlesinger F, et al. STAR: ultrafast universal RNA-seq aligner. *Bioinformatics*. 2013;29(1):15-21.
31. Liao Y, Smyth GK, Shi W. featureCounts: an efficient general purpose program for assigning sequence reads to genomic features. *Bioinformatics*. 2014;30(7):923-930.
32. Love MI, Huber W, Anders S. Moderated estimation of fold change and dispersion for RNA-seq data with DESeq2. *Genome Biol*. 2014; 15(12):550.
33. Sawant KV, Poluri KM, Dutta AK, et al. Chemokine CXCL1-mediated neutrophil recruitment: role of glycosaminoglycan interactions. *Sci Rep*. 2016;6:33123.
34. Deshmane SL, Kremlev S, Amini S, Sawaya BE. Monocyte chemoattractant protein-1 (MCP-1): an overview. *J Interferon Cytokine Res*. 2009;29(6):313-326.
35. Hoshiko S, Kawaguchi M, Fukushima T, et al. Hepatocyte growth factor activator inhibitor type 1 is a suppressor of intestinal tumorigenesis. *Cancer Res*. 2013;73(8):2659-2670.
36. Kawaguchi M, Kataoka H. Mechanisms of hepatocyte growth factor activation in cancer tissues. *Cancers*. 2014;6(4):1890-1904.
37. Wiesener MS, Jürgensen JS, Rosenberger C, et al. Widespread hypoxia-inducible expression of HIF-2α in distinct cell populations of different organs. *FASEB J*. 2003;17(2):271-273.

38. Tian H, Mcknight SL, Russell DW. Endothelial PAS domain protein 1 (EPAS1), a transcription factor selectively expressed in endothelial cells. *Genes Dev*. 1997;11(1):72-82.
39. Griffiths L, Binley K, Iqball S, et al. The macrophage—a novel system to deliver gene therapy to pathological hypoxia. *Gene Therapy*. 2000; 7:255-262.
40. Leek RD, Talks KL, Pezzella F, et al. Relation of hypoxia-inducible factor-2α (HIF-2α) expression in tumor-infiltrative macrophages to tumor angiogenesis and the oxidative thymidine phosphorylase pathway in human breast cancer. *Cancer Res*. 2002;62(5):1326-1329.
41. Henke N, Ferreirós N, Geisslinger G, et al. Loss of HIF-1β in macrophages attenuates AhR/ARNT-mediated tumorigenesis in a PAH-driven tumor model. *Oncotarget*. 2016;7(18):25915-25929.
42. Roda JM, Sumner LA, Evans R, Phillips GS, Marsh CB, Eubank TD. Hypoxia-inducible factor-2α regulates GM-CSF-derived soluble vascular endothelial growth factor receptor 1 production from macrophages and inhibits tumor growth and angiogenesis. *J Immunol*. 2011;187(4):1970-1976.
43. Acker T, Diez-Juan A, Aragones J, et al. Genetic evidence for a tumor suppressor role of HIF-2α. *Cancer Cell*. 2005;8(2):131-141.
44. Takeda N, O'Dea EL, Doedens A, et al. Differential activation and antagonistic function of HIF-{alpha} isoforms in macrophages are essential for NO homeostasis. *Genes Dev*. 2010;24(5): 491-501.
45. Shimomura T, Denda K, Kitamura A, et al. Hepatocyte growth factor activator inhibitor, a novel Kunitz-type serine protease inhibitor. *J Biol Chem*. 1997;272(10):6370-6376.
46. Owusu B, Galemmo R, Janetka J, Klampfer L. Hepatocyte growth factor, a key tumor-promoting factor in the tumor microenvironment. *Cancers*. 2017;9(4):35.
47. Gao CF, Woude GFV. HGF/SF-Met signaling in tumor progression. *Cell Res*. 2005;15:49-51.
48. Parr C, Watkins G, Mansel RE, Jiang WG. The hepatocyte growth factor regulatory factors in human breast cancer. *Clin Cancer Res*. 2004;10(1 Pt 1):202-211.
49. Ho-Yen CM, Jones JL, Kermorgant S. The clinical and functional significance of c-Met in breast cancer: a review. *Breast Cancer Res*. 2015;17(1):52-52.
50. Christensen JG, Burrows J, Salgia R. c-Met as a target for human cancer and characterization of inhibitors for therapeutic intervention. *Cancer Lett*. 2005;225(1):1-26.
51. Comoglio PM, Giordano S, Trusolino L. Drug development of MET inhibitors: targeting oncogene addiction and expedience. *Nat Rev Drug Discovery*. 2008;7(6):504-516.
52. Maroun CR, Rowlands T. The Met receptor tyrosine kinase: a key player in oncogenesis and drug resistance. *Pharmacol Ther*. 2014; 142(3):316-338.
53. Gherardi E, Birchmeier W, Birchmeier C, Woude GV. Targeting MET in cancer: rationale and progress. *Nat Rev Cancer*. 2012;12:89-103.
54. Kataoka H, Hamasuna R, Itoh H, Kitamura N, Koono M. Activation of hepatocyte growth factor/scatter factor in colorectal carcinoma. *Cancer Res*. 2000;60(21):6148-6159.
55. Parr C, Jiang W. Expression of hepatocyte growth factor/scatter factor, its activator, inhibitors and the c-Met receptor in human cancer cells. *Int J Oncol*. 2001;19(4):857-863.
56. Dykes SS, Hughes VS, Wiggins JM, Fasanya HO, Tanaka M, Siemann D. Stromal cells in breast cancer as a potential therapeutic target. *Oncotarget*. 2018;9(34):23761-23779.
57. Bhowmick NA, Neilson EG, Moses HL. Stromal fibroblasts in cancer initiation and progression. *Nature*. 2004;432(7015):332-337.
58. Yang H, Zhang C, Cui S. Expression of hepatocyte growth factor in breast cancer and its effect on prognosis and sensitivity to chemotherapy. *Mol Med Rep*. 2015;11(2):1037-1042.
59. Xiong Y, Russell DL, McDonald LT, Cowart LA, Larue AC. Hematopoietic stem cell-derived adipocytes promote tumor growth and cancer cell migration. *Int J Cancer Res Mol Mech*. 2017;3(1). https://doi.org/10.16966/2381-3318.130

SUPPORTING INFORMATION

Additional supporting information may be found online in the Supporting Information section.

How to cite this article: Susen RM, Bauer R, Olesch C, et al. Macrophage HIF-2α regulates tumor-suppressive Spint1 in the tumor microenvironment. *Molecular Carcinogenesis*. 2019; 58:2127–2138. https://doi.org/10.1002/mc.23103